Published January 30, 2014

Soil Physics

Determining the Diffusivity of Nitrous Oxide in Soil using In Situ Tracers

Iurii Shcherbak*
G. Philip Robertson
Michigan State Univ.
W.K. Kellogg Biological Station
3700 E. Gull Lake Dr.
Hickory Corners, MI 49060

Diffusion is a key process for understanding the movement of nitrous oxide (N_2O), carbon dioxide (CO_2), methane (CH_4), oxygen (O_2), and other biogeochemically important gases in soil. Soil gas diffusivity is highly variable, which makes the application of generic predictive models based on soil macrofeatures uncertain. In situ methods provide greater certainty but intensive sampling usually makes such determinations expensive. We compared single and inter-port diffusivity determinations using a sparse sampling alternative. We used 28 in situ profile probes with ports at five depths for pulse sulfur hexafluoride (SF_6) and N_2O tracer injections at single ports followed by two or three measurements in five adjacent ports at an agricultural site in southwest Michigan, USA. We repeated this procedure for three dates in the summer and two in the fall. In general, the sparse method provided accurate measurements of soil diffusivity. Estimated diffusivities of SF_6 and N_2O had poorer agreement in the summer (r^2 = 0.49) than in the fall (r^2 = 0.96), likely due to less uniform soil moisture in summer. The low N_2O to SF_6 diffusivity ratio (0.67 compared with 1.82 in free air) suggests that water solubility of N_2O plays a significant role in retarding its movement in the soil. Movement of the relatively insoluble SF_6 is not obscured by dissolution in water making SF_6 a superior tracer compared with N_2O. Median diffusivities in ports where the gas was injected were only moderately correlated (r^2 = 0.45) with diffusivities at the same depth measured by the inter-port method, likely due to an increase in the variability of diffusivity with distance from the injection port. Results show it is possible to estimate N_2O diffusivity with sparse measurements; accuracy can likely be further improved with knowledge of soil moisture and texture in the immediate vicinity of the injection and sampling ports, as uncertainty in water modeling is reduced.

Knowledge of soil gas dynamics is important for understanding soil aeration and the movement of greenhouse and other important gases in soil, and as well for parameterizing biogeochemical models used for predicting global change impacts (Li, 1992a, 1992b; Del Grosso et al., 2006) and contaminant flows (Moldrup et al., 2000; Resurreccion et al., 2010). Diffusion is the dominant process controlling soil gas movement (Jin and Jury, 1996; Werner et al., 2004). It is the result of the random movement of gas molecules and tends to equilibrate gas concentrations without requiring mass flow.

Diffusion is usually characterized with a diffusivity or diffusion coefficient, which is a proportionality constant that connects the gas concentration gradient with diffusive flux (Lide, 2010). The diffusivity coefficient is central to gas dynamics models, and in recent decades much effort has been devoted to developing practical and theoretical methods for measuring and estimating diffusivity under various conditions in undisturbed and repacked soils in the laboratory and in the field.

Supplemental material available for this article online.
Soil Sci. Soc. Am. J. 78:79–88
doi:10.2136/sssaj2013.05.0181
Received 14 May 2013.
*Corresponding author (yurann@gmail.com).

Most laboratory methods to measure the diffusivity coefficient employ a repacked or intact soil column that has injection and sampling ports along the column sampled 10–15 times over an injection period (Allaire et al., 2008). Diffusivity is then calculated either as the rate of gas disappearance from the injection chamber or as the rate of gas accumulation at the opposite end. While relatively straightforward, for repacked soil columns this method does not account for in situ diffusion through macropores that are destroyed on repacking and that can otherwise have a big influence on total diffusivity (Lange et al., 2009). Even intact soil columns are usually not large enough to include all macro features (Allaire and van Bochove, 2006). This problem can be partly alleviated by instead measuring diffusion in intact soil monoliths in the lab (>0.5 m on a side, Allaire et al., 2008). Monoliths are more difficult to keep at constant moisture, however, and are very labor and cost intensive, especially for heterogeneous sites. Large monoliths also cannot be readily replicated.

In situ field methods provide an attractive alternative that do not suffer from distorted macropore or other soil structure issues associated with laboratory determinations. Field measurements of gas diffusivity reviewed by Werner et al. (2004) examine flux chamber, atmospheric tracer, instantaneous point-source single-port, instantaneous point source inter-port, and continuous point source inter-port methods. The flux chamber method consists of a chamber that is placed with edges a few centimeters into the soil and that is then injected with a tracer gas. The tracer diffuses into the soil at a rate estimated by its disappearance from the chamber. This method works well for short measurement intervals and provides diffusivity measurements in soil surface layers.

The atmospheric tracer method (Weeks et al., 1982) relies on gas concentrations measured at several depths in the soil profile and historical gas concentrations in the atmosphere to estimate diffusivity. A one-dimensional diffusion equation uses atmospheric gas concentration at the surface and no flux at the water table as boundary conditions. The method is simple to implement as only two measurements at each depth are required, but is limited to environments where gases move very slowly, are not biologically active, and do not express large temporal or spatial variations.

Table 1. Relative soil gas diffusivity (D_p/D_o) models following the Buckingham–Currie power-law function. Model references are as compiled in Jassal et al. (2005) and Resurreccion et al. (2010).

Model	Formula†
Buckingham (1904)	ε^2
Penman (1940)	0.66ε
Millington (1959)	$\varepsilon^{4/3}$
Marshall (1959)	$\varepsilon^{1.5}$
Millington and Quirk (1960)	$\varepsilon^{10/3}/\Phi^2$
Millington and Quirk (1961)	$\varepsilon^2/\Phi^{2/3}$
Moldrup et al. (2000)	$\varepsilon^{2.5}/\Phi$
Jassal (2005)	$1.18\varepsilon^{2.27}$
Moldrup et al. (2005)	$\varepsilon^{X_{100}}\Phi^{2-X_{100}}$ $X_{100}=2+0.25\ln\varepsilon_{100}/(\ln\varepsilon_{100}-\ln\Phi)$
Cannavo et al. (2006)	$1.12\varepsilon^{2.13}$

† ε is the soil air content, ε_{100} is soil air content at -100 cm of matric potential, Φ is the total porosity.

The instantaneous point-source single-port method (Lai et al., 1976) uses the same port to introduce a tracer and remove samples. Diffusivity is calculated by analytical or numerical methods. The method is relatively simple to implement and analyze and requires low numbers of samples, but the measurement volume is poorly defined and some probe designs can disturb the soil during installation. These limitations make the method useful for fast determinations of diffusivity, but many sampling ports are required because of sampling volume uncertainty.

The instantaneous point-source inter-port method (Nicot and Bennett, 1998; Werner and Hohener, 2003) uses two or more ports. One is used for injection and others are sampled to determine the time to maximum concentration at different distances from the injection port. A better defined sampling volume allows fewer probes to estimate diffusion, but the method requires frequent sampling due to high sensitivity of diffusivity estimates to the time it takes gases to reach maximum concentration at some distance from the injection point.

The continuous point-source inter-port method (Kreamer et al., 1988) also uses several ports, but the tracer is released from the injection port at a constant rate. This method allows for much simpler steady-state solutions to obtain the diffusivity constant and is presently the most reliable field-based method. However it requires that significant amounts of tracer be injected at a constant rate for long periods (up to several days depending on the inter-port distances), and that soil conditions do not significantly change before steady state is achieved for the soil volume of interest.

Attempts have also been made to predict gas diffusivity from static soil characteristics that are more readily available or estimable. Most models of soil diffusivity use total soil porosity (Φ), the volume of air (ε), and pore geometry (tortuosity and connectivity) and have the general form $a\varepsilon^b\Phi^{-c}$, where a, b, and c are numerical constants that account for pore geometry and are used to bring the model into agreement with the data (Table 1). Other models distinguish between inter- and intra-aggregate porosity and use more complicated relationships of diffusivity to soil characteristics, often additionally requiring knowledge of soil air volume at one or more matric potentials (e.g., ε_{100}, air volume at −100 cm H_2O pressure head; Moldrup et al., 2005) and representing diffusivity with a piecewise function where pieces relate to intervals of the water-filled porosity (Resurreccion et al., 2010).

Despite much effort, a universal predictor of diffusivity for many soil types and conditions has not been found (Jin and Jury, 1996). Bruckler et al. (1989) concluded that such a predictor cannot exist because it would necessarily be dependent on complex pore geometry, which might not be possible to represent with soil parameters that are easily measured. For any given site large differences in diffusivities are obtained by different models and it is difficult to select the best one for the site on purely theoretical grounds. Many diffusivity models are also very sensitive to air filled and total porosity since they are raised to high pow-

ers in many popular models (Werner et al., 2004). Thus model selection for any given site is probably best informed by in situ measurements at the site of application using equipment that is easy to install and operate.

Here we describe an inexpensive soil profile atmosphere probe that can be used for in situ measurements of gas concentrations to yield diffusivity as a numeric solution of the diffusion equation. Our specific objectives are (i) to test the applicability of in situ tracer measurement to determine diffusivity with inverse methods, (ii) to test if measurements made with SF_6 are more appropriate than direct measurements with N_2O, and (iii) to evaluate the effectiveness of single port vs. inter-port methods. To address the second objective we also measured N_2O consumption at depth. We then compare measured diffusivities against values provided by models from the literature.

MATERIALS AND METHODS

Site Description

We measured diffusivities at the Resource Gradient Experiment at the W.K. Kellogg Biological Station Long-Term Ecological Research Site (KBS LTER; http://www.kbs.msu.edu/research/lter; accessed 12 Dec. 2013), located in southwest Michigan in the northeast portion of the U.S. Corn Belt (42° 24′ N, 85° 24′ W, with average elevation 288 m). Mean annual temperature is 10°C and annual rainfall averages 1027 mm yr^{-1} with about half of the precipitation received as snow. Detailed weather and soil data for the 2011 growing season are in the online supplemental material Fig. S1, S2, and S3. Soils are a mixture of Kalamazoo (fine-loamy, mixed, semi-active, mesic Typic Hapludalfs) and Oshtemo (coarse-loamy, mixed, active, mesic Typic Hapludalfs) loams (Mokma and Doolittle, 1993; Crum and Collins, 1995) (Table 2).

The KBS LTER Resource Gradient Experiment provides a range of N fertilization levels under both rainfed and irrigated conditions in a corn (*Zea mays* L .)–soybean (*Glycine max* L.) –wheat (*Triticum aestivum* L.)rotation. Experiments were performed in summer and fall 2012 with the field planted to soybean. Planting occurred on May 22 at 45 seeds m^{-2} in 38 cm rows to a depth of 4 cm. Plots are 4.6 by 27.4 m arranged four replicate blocks. In this study we used plots with 56 and 74 kg N ha^{-1} in rainfed plots and 37 and 93 kg N ha^{-1} in irrigated plots in one block.

Soil Profile Gas Sampling

We used five-port soil profile gas probes to make tracer injections at different soil profile depths and to collect gas samples, which we then used to determine diffusivities. We compared diffusivities across treatments, injection depths, and seasons. We also compared measured diffusivities with the diffusivities from published models.

Our five-port soil profile gas probe (Fig. 1) consists of a master tube made of stainless steel (90 cm long, ~6.4 mm o.d., and ~4.8 mm i.d.) that contains five stainless steel sampling tubes (~1.6 mm o.d. and 0.5 mm i.d.) that protrude 3 cm from the outer walls of the master tube at the 12-, 24-, 36-, 60-, and 90-cm depths. Openings around the protrusions are sealed with airtight silicon-based sealant to prevent gas diffusion into and out of the master tube. The upper ends of the sampling tubes each fitted with a brass reducer (Swagelok, Solon, OH) and rubber septum for sampling access. The largest dead space for the port at the 90-cm depth is about 1 mL.

To minimize the impact on future tracer concentrations, the protocol minimized the volume of gas taken. To draw a sample, we pierced a septum with a needle attached to a syringe and pumped the air inside the tube three times by drawing 10 mL of air and immediately injecting it back into the port. Then we injected 5 mL of soil gas sample and 5 mL of atmospheric air to a 5.9-mL non-evacuated Exetainer vials originally containing air at atmospheric pressure to create overpressure. Samples were analyzed for N_2O and SF_6 as described above.

Table 2. Kellogg Biological Station Long-Term Ecological Research Site soil textures (Kalamazoo and Ostemo Series). Texture is based on percentage of fraction <2 mm (from Crum and Collins, 1995). The pH values assume no liming is performed at the site.

			Texture								
Horizon	Depth	Color	Sand	Silt	Clay	Texture	CEC	Total C	Total N	pH	Bulk density
	cm						cmol(+)kg^{-1}	g kg^{-1}			Mg m^{-3}
Kalamazoo series: Fine-loamy, mixed mesic Typic Hapludalfs											
Ap	0-30	10YR 3/3	43	38	19	Loam	8.4	12.85	1.31	5.5	1.6
E	30-41	7.5YR 5/4	39	41	20	Loam	11.5	3.25	0.53	5.7	1.7
Bt1	41-69	7.5YR 4/6	48	23	29	Sandy clay loam	15.3	2.25	0.42	5.3	1.8
2Bt2	69-88	7.5YR 4/6	79	4	17	Sandy loam	4.1	0.67	0.42	5.2	nd
2E/Bt	88-152	(E)10YR 6/4 (B)7.5YR 4/6	93	0	7	Sand	2.3	0.2	0.18	5.6	nd
Oshtemo series: Coarse-loamy, mixed, mesic Typic Hapludalfs											
Ap	0-25	10YR 3/3	59	27	14	Sandy loam	7.1	9.67	1.04	5.7	1.6
E	25-41	7.5YR 5/4	64	22	14	Sandy loam	6.8	2.52	0.43	5.7	1.7
Bt1	41-57	7.5YR 4/4	67	13	20	Sandy clay loam	8.1	1.99	0.4	5.8	1.8
2Bt2	57-97	7.5YR 4/6	83	4	13	Sandy loam	6.4	1.28	0.53	5.8	nd
2E/Bt	97-152	(E)10YR 6/4 (B)7.5YR 4/6	92	0	8	Sand	2.4	0.25	0.18	6	nd

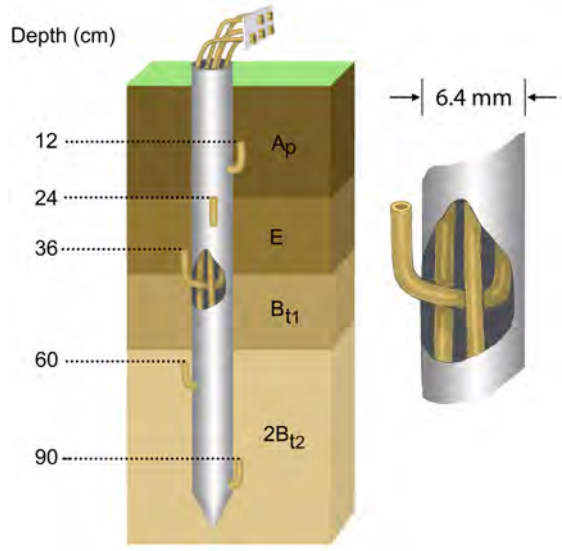

Fig. 1. Soil profile gas probe with ports at the 12-, 24-, 36-, 60-, and 90-cm depths. Diameter of the probe is 6.4 mm and is not shown to scale.

Nitrous Oxide Consumption in the Soil

We performed microcosm experiments to determine the suitability of using N_2O directly as a non-consumable tracer for soil diffusivity determinations. If N_2O is consumed then it cannot be used to measure diffusivity reliably.

On 25 May 2012 we took one sample of the 0- to 10-cm soil from the first four replicates of soybeans in the Conventional, No-till, Reduced input, and Biologically based systems, and Alfalfa, Poplar Early Successional, and Mown Grassland (never tilled) systems at the Kellogg Biological Station (KBS) Long-Term Ecological Research Site, <500 m from the soil gas probe installations on the same soil type. Soil samples were put through a 4-mm sieve. Moisture contents of the soil were estimated by drying subsamples in an oven at 105°C. The next day two 200-g fresh weight subsamples were placed in a 1-L mason jar (Jarden, Rye, NY). We added 75 mL of deionized water to completely saturate the soil, with one subsample receiving nitrate at 150 mg N kg^{-1} soil. Jars were then sealed with lids with septa to allow for gas sampling and to each jar was added 1 mL of 45 nmole L^{-1} SF_6 (1 ppm_v) and 1 mL of 2.23 mmole L^{-1} N_2O (5% by volume). An additional 60 mL of laboratory air were added to each jar to create an initial overpressure. Headspace samples were taken 12, 24, 48, 72, 96, and 120 h after the jars were sealed. At each sampling we removed 5 mL of microcosm atmosphere to a 5.9-mL non-evacuated Exetainer vial (Labco Ltd., High Wycombe, UK) to which we then added 5 mL of air to over-pressurize during storage. Samples were analyzed within 10 d of collection.

Again, on 10 Oct. 2012, we took duplicate 6-cm diameter 1 m-deep soil cores from two rainfed and two irrigated locations on the Resource Gradient site with a hydraulic sampler (Geoprobe, Salina, KS). The locations of these samples were <2 m from corresponding soil gas probe installations as explained below. The next day, three 300-g field moist samples from each core at depths 5 to 25, 35 to 50, and 75 to 90 cm were sieved and placed in duplicate jars that were then supplemented with 75 mL of deionized water and injected with SF_6 and N_2O as described above. We took a total of nine headspace samples per jar 0, 4, 8, 13, 19, 27, 37, 50, and 74 h after the jars were closed.

Samples were analyzed for SF_6 and N_2O using a gas chromatograph (Aglilent 7890A, Aglilent Technologies, Wilmington, DE) equipped with an auto-sampler (Gerstel MPS 2 XL, Gerstel Inc., Linthicum, MD). Sulfur hexafluoride and N_2O were separated with one of two Restek PP-Q 80/100 packed columns (length 3 m, i.d. 2 mm, o.d. 3.175 mm. Restek Corp., Bellafonte, PA) and detected using a ^{63}Ni electron capture detector at 350°C. Carrier gas was 90% Ar and 10% CH_4 (Ultra High Purity Grade 5.0 with a Restek 21997 moisture trap and Restek 20601 oxygen scrubber) at a 10 ± 0.5 mL min^{-1} flow rate. Oven temperature was 78°C during the first 5.5 min of the run, and then the column was back flushed and baked for 0.5 min (terminal temperature 105°C, increase rate 55°C min^{-1}). The analytical coefficient of variation was below 2% for SF_6 and N_2O.

Tracer Injection and Data Collection

We installed 28 soil profile gas probes in Block 1 of the Resource Gradient Experiment. Seven probes were installed in each of two replicate rainfed and two replicate irrigated plots. Every probe was installed into a predrilled vertical well made with a 6.35 mm × 0.9-m length drill-bit (Model A36.250; Associated Industrial Distributors, Crystal Lake, IL). Sampling depths were 12, 24, 36, 60, and 90 cm (Fig. 1). The seven probes per plot were installed in a configuration designed to check diffusivity not only in the vertical but also in the horizontal direction (Fig. 2). We used two of the probes for gas injection at the 90-cm depth, two for gas injection at the 60-cm depth, one probe for gas injection at the 36-cm depth, and two control probes were not used for gas injection. Probes were located at least 3 m from a plot edge. Each pair of probes used for injection at 60 and 90 cm was grouped with a control probe to form an equilateral triangle with 0.9 m side (Fig. 2) so that the concentrations at the horizontal distance from the injection port could be measured. Installations were performed separately for summer and fall in the same plots with probes installed into a well of the same diameter at least 10 d before first sampling to allow soil to equilibrate post-installation and provide a good seal between sampling ports.

Experiments were performed over five dates in 2012: three in the summer (June 20, June 27, and July 03) starting 29 d after planting, and two in the fall (Oct. 29 and Nov. 1) shortly after harvest. Summer sampling occurred after 3 wk without rain, whereas fall experiments followed about 14 cm of rain during October, which completely recharged the profile as it holds 12 cm of water per meter. On each sampling date we sampled ports used for gas injection to determine background concentrations of N_2O and SF_6. Direct measurement of baseline tracer concentrations eliminated the need to measure concentration of the precursors: nitrate and soluble organic C. We injected 2 mL of 45 nmole L^{-1} SF_6 (1 ppm_v) and later 2 mL of 44.6 mmole L^{-1} N_2O (100% by volume) into the injection port with each gas

followed by 8 mL of atmospheric air to flush the dead volume of the injection ports. Injections of each gas into 20 injection ports took about 10 min to complete. Following the injections, we took three sets of samples: (i) from 20 injection ports (taking 15 minutes), (ii) from all 140 ports (taking 60 min.), (iii) from all 140 ports (taking 60 min.). We allowed 15 min between the sampling sets. We obtained four independent diffusivity estimates for the 36-cm injection depth, and eight estimates for the 60- and 90-cm injection depths. A total of 20, 40, and 40 diffusivity values for injection depths at 36, 60, and 90 cm have been obtained, respectively.

Diffusivity Calculations

We estimated layered soil water content and temperature with the SALUS (System Approach to Land Use Sustainability; Basso et al., 2006) model, parameterized and tested for the site earlier (Senthilkumar et al., 2009, Syswerda et al., 2012). We validated modeled averages for the 0- to 25-cm soil depth with measured data for the same depth. We did not measure particle density and assumed it is 2.65 g cm^{-3}. To calculate porosity we assumed bulk density below 69 cm stayed the same at 1.8 g cm^{-3}. Using total porosity and modeled water content we estimated air-filled porosity (ε) to be used in diffusivity calculations.

We obtained diffusivity by numerical procedure performing an interval search for diffusivity value minimizing the sum of squared differences of measured tracer concentrations and tracer concentrations from the diffusion equation for the same position in space and time. The general form of a nonhomogeneous three-dimensional diffusion equation in cylindrical coordinates is

$$\frac{\partial(\varepsilon C)}{\partial t}=\frac{1}{r}\frac{\partial}{\partial r}\left(Dr\frac{\partial C}{\partial r}\right)+\frac{1}{r^2}\frac{\partial}{\partial \varphi}\left(D\frac{\partial C}{\partial \varphi}\right)+\frac{\partial}{\partial z}\left(D\frac{\partial C}{\partial z}\right)+g \qquad [1]$$

where r is the radius, j is the angular coordinate, z is the vertical coordinate, e is the fraction of air-filled porosity, $D = D(r, j, z)$ isthe diffusivity of gas, $g = g(t, r, j, z)$ production function, concentration of gas.

Because there was no production or consumption of SF_6 or N_2O (see Results) we assumed angular symmetry of concentrations. We assumed diffusion was constant at the same depth. We assumed porosity to stay constant for each depth for the duration of the experiment. Therefore, the equation simplifies to the two-dimensional homogeneous form

$$\varepsilon\frac{\partial C}{\partial t}=\frac{D}{r}\frac{\partial}{\partial r}\left(r\frac{\partial C}{\partial r}\right)+\frac{\partial}{\partial z}\left(D\frac{\partial C}{\partial z}\right) \qquad [2]$$

Initial concentrations were assumed to follow the two dimensional error function

$$C_{0,r,z}=\frac{vC_{inj}}{2\pi\sigma^2}e^{-\frac{1}{2\sigma^2}\left[r^2+(z-z_0)^2\right]} \qquad [3]$$

where $C_{0,r,z}$ is the initial concentration at point (r, z), C_{inj} and V_{inj} are concentration and volume of the gas injected, respectively, s a parameter equal to 4 cm, $(0, z_0)$ is the point of injection, v, parameter, adjusted so that $\iint rC_{0,r,z}\,dr\,dz=V_{inj}C_{inj}$.

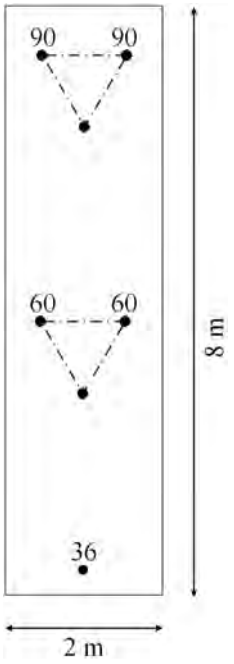

Fig. 2. Replicate (top view) consists of seven soil profile gas probes arranged in two equilateral triangles with 90 cm sides and an additional injection sampler. Values above probes indicate port used for gas injection (in addition to sampling). Unmarked probes were used for sampling only.

Concentrations at the border were assumed to be 0 at all times. The exact initial distribution is inconsequential, since the first sampling occurs at least 15 min after the injection and there were no abrupt changes in concentrations. In a general case this equation with initial and boundary conditions does not have an analytical solution, so we employed the alternating direction implicit method (Peaceman and Rachford, 1955). Equations that describe the process are

$$\varepsilon_j\frac{C_{i,j}^{n+\frac{1}{2}}-C_{i,j}^{n}}{\Delta t/2}=\frac{D_j}{r_i}\delta_r C_{i,j}^{n+\frac{1}{2}}+D_j\delta_{rr}C_{i,j}^{n+\frac{1}{2}}+\delta_z D_j\delta_z C_{i,j}^{n}+D_j\delta_{zz}C_{i,j}^{n} \qquad [4]$$

$$\varepsilon_j\frac{C_{i,j}^{n+1}-C_{i,j}^{n+\frac{1}{2}}}{\Delta t/2}=\frac{D_j}{r_i}\delta_r C_{i,j}^{n+\frac{1}{2}}+D_j\delta_{rr}C_{i,j}^{n+\frac{1}{2}}+\delta_z D_j\delta_z C_{i,j}^{n+1}+D_j\delta_{zz}C_{i,j}^{n+1} \qquad [5]$$

where $C_{i,j}^{n}$ concentration at time $n\Delta t$, at radius $i\Delta r$, and depth $j\Delta z$, Δr is step in radial direction, Δz, is the step in vertical direction, Δt is the time step, $\delta_z D_j=(D_{j+1}-D_{j-1})/(2\Delta z)$, $\delta_r C_{i,j}=(C_{i+1,j}-C_{i-1,j})/(2\Delta r)$, $\delta_{rr}C_{i,j}=(C_{i+1,j}-2C_{i,j}+C_{i-1,j})/(\Delta r)^2$, $\delta_z C_{i,j}=(C_{i,j+1}-C_{i,j-1})/(2\Delta z)$, $\delta_{zz}C_{i,j}=(C_{i,j+1}-2C_{i,j}+C_{i,j-1})/(\Delta z)^2$.

The equations were run in a cycle from time 0 to T with a step Δt, where during each iteration diffusion is assumed to occur in a horizontal direction for the first equation and in a vertical direction for the second. During time step $n+1$, terms from previous time steps $n+1/2$ and n are considered known. Assembling unknown terms on the right-hand side yields a set of tridiagonal

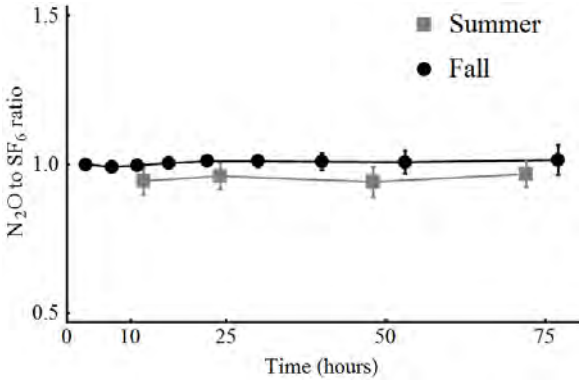

Fig. 3. Mean N_2O to SF_6 ratio over time in summer and fall microcosm experiments. Only microcosms retaining more than 60% of original SF_6 have been retained. Error bars are lower and upper boundaries of the 95% confidence interval for the median.

matrices that are solved (Thomas, 1949) to find concentrations in the next time step.

We fit diffusivity parameters to the data using a program written in C#.NET 4.5 (Microsoft, 2012; see supplemental materials for source code). The program executed a search in diffusivity parameter space with an objective function to minimize the sum of squared deviations between measured and simulated gas concentrations. Diffusivities ranged from 10^{-9} to 1.38 10^{-5} m^2 s^{-1}, with limits of diffusivity being diffusivity in water and in air, respectively. We ran the diffusivity adjustment model involving only the region with the injection port for both N_2O and SF_6 and compared them.

We performed parametric (two-sided *t* test) comparisons of diffusivities obtained for injection ports by depth, presence of irrigation and time of year (summer or fall). For the 60- and 90-cm depths, we compared SF_6 diffusivities for ports used for injections with median values of diffusivities for ports at the same depth that were only used for sampling. Statistical analyses were performed in Wolfram Mathematica 9.0 (Wolfram Research, 2012).

We performed full five-port probe diffusivity adjustment for N_2O and SF_6. The parameter space in each case consisted of independent diffusivities for consecutive layers with borders at 0, 18, 30, 41, 69, and 120 cm. A 4-cm border region between every two layers has diffusivity as a linear mixture of the layers. We compared diffusivities for injection ports in this procedure (full diffusivity) with corresponding injection port diffusivities in simplified procedure (one-port diffusivity). We then used resampling to compare median diffusivity of ports not used for gas injection (sampling port diffusivity) with median diffusivity of ports used for injection at the same depth (injection port diffusivity).

Using moisture content, temperature, and texture as inputs we obtained diffusivities using existing soil diffusivity models (Table 1) and compared those with diffusivities we obtained by our method.

RESULTS

Nitrous Oxide Consumption Experiment

Headspace concentrations of N_2O relative to the inert tracer SF_6 did not significantly decline for the duration of the experiment, 77 h, in experiments with soil samples taken either in summer or fall (Fig. 3): measured N_2O consumption was nil. We had to remove approximately half of the microcosm replicates where more than 40% of original SF_6 content was lost from a jar due to a defective seal; the remaining dataset had significantly reduced variance.

Field Experiments

Figure 4 compares diffusivity estimates for decreasing concentrations of injected N_2O to those for SF_6 for summer and fall samplings. Sulfur hexafluoride diffusivities have much better agreement with the concentration measurements (only 5% of runs have $r^2 < 0.85$) than N_2O diffusivities (60% of runs did not achieve $r^2 < 0.85$). We have removed 6 SF_6 diffusivity results with $r^2 < 0.85$ and 17 N_2O diffusivity results with $r^2 < 0.6$. However, SF_6 and N_2O diffusivities agreed reasonably well (Fig. 4a, $r^2 = 0.64$) when calculated only on remaining experiments. By season, SF_6 diffusivities were only weakly correlated with N_2O diffusivities in the summer experiments (Fig. 4b, $r^2 = 0.53$), while SF_6 and N_2O diffusivities had very high agreement in the fall experiments (Fig. 4c, $r^2 = 0.95$). The N_2O to SF_6 diffusivity ratio for the fall experiments was 1.24.

Diffusivities of SF_6 in the rainfed treatments were significantly ($p < 0.02$) higher than respective values for irrigated treat-

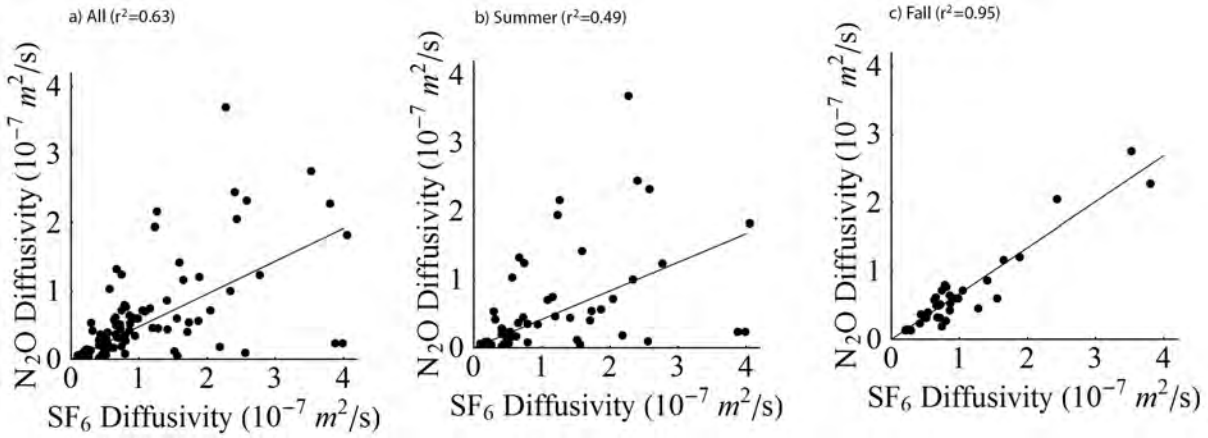

Fig. 4. Comparison of SF_6 and N_2O diffusivities. Each replicate observation is a separate point. Straight line is the regression line with best slope through the origin.

ments for all depths in summer tests (Fig. 5) while differences for diffusivities at the 90-cm injection depth were also significant for the fall samples. Nitrous oxide diffusivities had similar differences between respective rainfed and irrigated treatments, but larger variability and exclusion of some diffusivity values led to weaker results (p = 0.10– 0.15). The soil layers show a declining difference between rainfed and irrigated treatment diffusivities with depth. Diffusivities of SF_6 in the rainfed treatment significantly declined with depth (p < 0.03) in the summer, with the first sampling date having a lower significance at p = 0.1.

Sulfur hexafluoride diffusivities involving only the injection port almost perfectly coincided with diffusivities for the injection port obtained from full scale simulations (Fig. 6 a, r^2 = 0.99). Single-port vs. inter-port SF_6 diffusivity comparisons yielded a weak correlation (Fig. 6 b, r^2 = 0.4). Nitrous oxide diffusivities followed the same trends, but are much more variable and do not show significant differences.

In our experiments models of diffusivity based on soil moisture content do not have strong predictive ability for diffusivities since they all use soil moisture as a main predictor, which is only weakly correlated with our diffusivity measurements (Fig. 7).

DISCUSSION

Overall results suggest that the point source single port method is adequate for diffusivity measurements and that the point source inter-port method does not improve results (as noted in Fig. 6b) despite a better defined sampling volume. We also found that diffusivity is not easily measured directly with N_2O due to its greater solubility in water. Sulfur hexafluoride with its lower solubility is a superior tracer, which movement is not obscured by absorption and release by soil water. Sulfur hexafluoride diffusivity can be converted to N_2O diffusivity based on their mass differences.

Nitrous Oxide Consumption

Nitrous oxide (N_2O) dynamics in soil depends on its diffusion between the layers, as well as production and consumption of the gas. To use N_2O directly as a diffusivity tracer requires that N_2O dynamics be determined only by diffusion and not be lost or gained in the layers via biological activity. Nitrous oxide production in soil can be significant, but is not an obstacle for short-term experiments because background concentrations usually change slowly and can be measured at the beginning of the experiment. Nevertheless, it is necessary to show that N_2O consumption in a given soil is insignificant in situ; otherwise measurements of diffusion could be an artifact of substantial N_2O consumption.

The ability of soils to consume N_2O has only been tested for a limited range of soil types and no comprehensive survey exists (Clough et al., 2005). While many researchers have found evidence for N_2O consumption in laboratory experiments (Goldberg and Gebauer, 2009), others have not (van Bochove et al., 1998). Some field experiments have a significant number of small negative fluxes that might indicate the possibility of consumption, but other explanations have been proposed as well. Interactions of N_2O with water complicate the in situ determinations of N_2O consumption at depth (Heincke and Kaupenjohann, 1999).

Concentrations of N_2O relative to SF_6 did not decline in our laboratory incubations with soil samples taken in summer or fall (Fig. 3) regardless of profile depth and even under optimal consumption conditions of a mixed slurry. This indicates that N_2O was not consumed to a measureable degree. This result allows us to consider using N_2O as an inert tracer for our short-term (<5 h) and possibly longer in situ diffusivity experiments for these soils.

Diffusivity of Soluble Gas

Water content is a major determinant of gas diffusivity in soil. Its influence becomes even more complex when the gas of interest is soluble (e.g., N_2O) or reacts with water to form other compounds (e.g., CO_2). Below we derive a theoretical ratio of apparent diffusivities of two gases with different masses and solubility under equal concentration gradients and soil conditions. For equal gradients of concentrations in air or soil (if solubility and reactions with water can be ignored) two gases have the ratio of fluxes and diffusivities approximately inversely proportional to the square root of their molar mass ratio ($D_2/D_1 \sim \sqrt{M_1/M_2}$). For example, for N_2O/SF_6 this ratio is 1.82 (SF_6 and N_2O masses are 146 and 44 g mol^{-1}, respectively). Differences in the solubility of gases modify this relationship. To derive an adjustment factor for the diffusivities of the two gases with solubility f_1 and f_2 (expressed as Bunsen absorption coefficients or ratios of equilibrated gas concentrations in water to concentration in the headspace) we assume that both gases achieve instantaneous equilibrium between air (a) and water (w) fractions of total porosity. The flux of the gas through the air-filled phase depends only on the concentration gradient and not the solubility. Since soluble gas has ($a + f_i w$) of combined gas in water and air phases, the change in concentration will be slower by a factor $a/(a + f_i w)$ compared with an insoluble gas (f_i= 0) of the same molar mass. Since apparent diffusion is proportional to observed change in concentrations, the ratio of diffusivities (D_i) of the two gases is

$$\frac{D_2}{D_1} = \sqrt{\frac{M_1}{M_2}}\,\frac{a + f_1 w}{a + f_2 w} \qquad [6]$$

Heincke and Kaupenjohann (1999) have reviewed in detail other factors that influence N_2O solubility, including temperature, salt concentration and type, pH of the solvent, and possibly dissolved organic matter. Clay content can also influence apparent solubility through adsorption effects.

Diffusivities Measured by Sulfur Hexafluoride and Nitrous Oxide Tracers

For SF6 only 5% of the measured diffusivities had an r^2 < 0.85, whereas for N_2O over 60% of diffusivities lacked this fit. This difference is likely due to heterogeneous distribution of soil water that influences the diffusion of N_2O because of its relative-

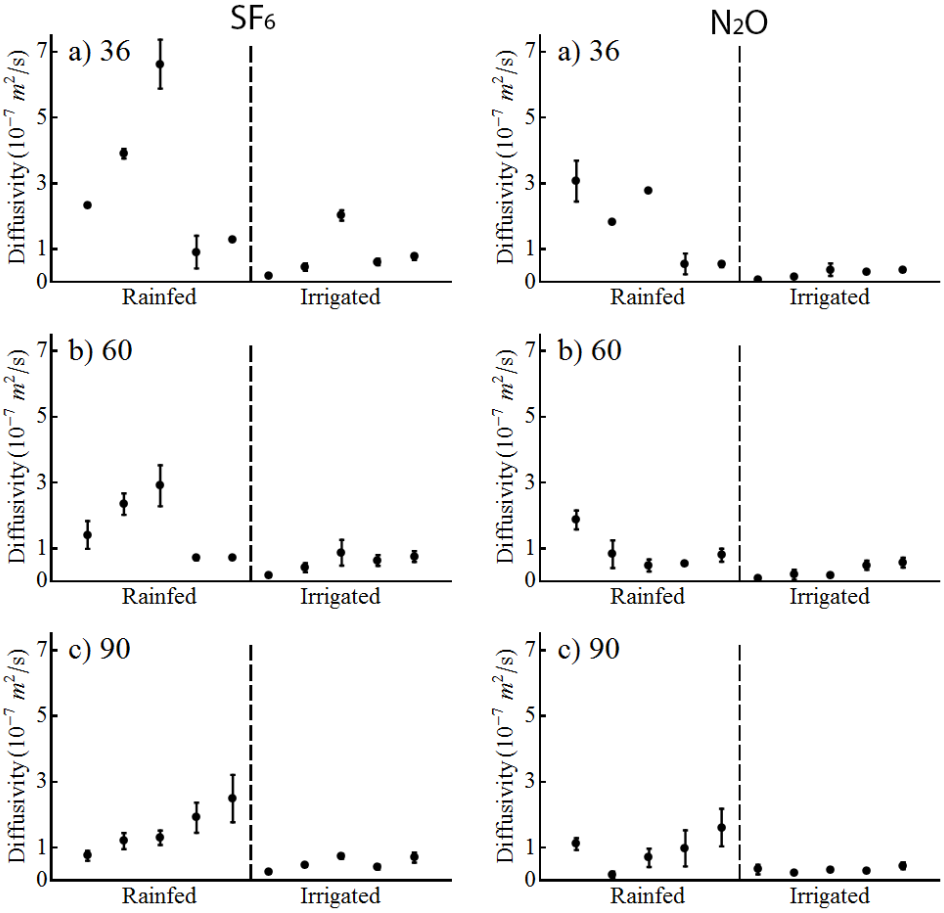

Fig. 5. Sulfur hexafluoride and N_2O diffusivities modeled for ports used for injections. Sulfur hexafluoride is in the left column and N_2O is in the right column. Treatments are Rainfed and Irrigated. Within each treatment there are values for five experimental dates arranged chronologically: June 20, June 27, July 03, October 29, and November 1. Only diffusivities with R^2 above 0.85 for SF_6 and 0.6 for N_2O are included.

ly high solubility of 1.47 g L^{-1} (Gevantman, 2010) as compared with SF_6's solubility of 0.036 g L^{-1} (Friedman, 1954).

Diffusivities of SF_6 and N_2O are highly correlated for the fall measurements but only weakly correlated for the summer. This is likely due to differences in soil moisture. Heterogeneity of the water content is caused by variation of soil physical properties (texture, aggregation, porosity), precipitation, and temperature (Allaire et al., 2008). During the growing season variation in water content is increased due to the heterogeneous distribution of roots; this variation is present in both rainfed and irrigated treatments, despite the higher overall water content in the irrigated treatment.

The slope of the best-fit line for the ratio of N_2O and SF_6 diffusivities combines the effects of mass and solubility differences and possible other differences in their interaction with the medium. The lower slope of only 0.67 for fall (Fig. 4) compared with the ratio of diffusivities in free air indicates that the high solubility of N_2O has a major influence on its apparent diffusivity. Fall diffusivity ratios of N_2O and SF_6 are consistent because water content was more uniform after the soil profile had been recharged and no plant uptake influenced the distribution of water. Substituting measured diffusivity ratio, molar mass ratio, and air-filled porosity (1–10% modeled in SALUS) into Eq. [6] we obtain the ratio of water to air N_2O concentrations of 0.1 to 0.6 (at 32–40% porosity based on a bulk density of 1.6–1.8), a value that is lower than equilibrium partitioning (0.6–0.8 at temperatures of 13–23°C). This suggests that N_2O is a poor choice of tracer gas, since it behaves differently from N_2O produced in soil that is in equilibrium with soil water. This might not be true for air-filled porosity values above 10%, where N_2O will be more in equilibrium with water, behaving similarly to N_2O produced in the soil. Therefore, using SF_6 as a tracer gas and then applying modifications to adjust diffusivity for mass and solubility differences between SF_6 and N_2O (or another soluble gas of interest) is a more appropriate strategy for soils with low air-filled porosity.

Diffusivities of Rainfed and Irrigated Treatments

Comparing SF_6 and N_2O diffusivities from rainfed and irrigated treatments (Fig. 5) agrees with the general prediction that diffusivity will grow with air-filled porosity since the diffusivity of gases in air is usually several orders of magnitude greater than their diffusivity in water. So, a larger diffusivity in rainfed compared with irrigated treatments in the summer is likely due to the greater percentage of soil pores occupied by air in the rainfed treatment. The irrigated treatment did not receive any additional water after the summer, so its water content was mostly equilibrated and diffusivity differences between the two treatments that were present in the summer disappeared in the fall, except for the deepest layer, which was not completely saturated by November in the rainfed treatment. Smaller differences between SF_6 and N_2O diffusivities of rainfed and irrigated treatments in deeper layers are likely also caused by a similarity in water content even in the summer due to the relative scarcity of roots at the 90-cm depth. The decrease in SF_6 diffusivities of rainfed treatment in the summer are also caused by the modeled decrease in air-filled porosity with depth.

Single-Port vs. Inter-Port Diffusivities and Comparison with Models

Diffusivities for ports not used for injection have much higher variability than diffusivities for ports used for gas injection. The main reason for this is that spatial variability compounds with more layers between injection and measurements (Fig. 6).

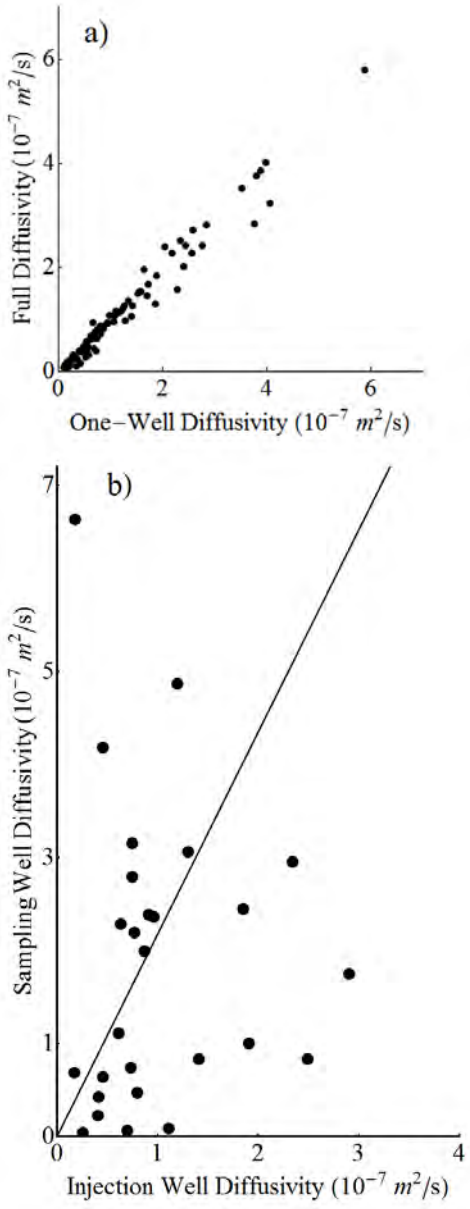

Fig. 6. Comparison of SF_6 diffusivities obtained from simulations involving only ports used for tracer injections with (a) corresponding diffusivities for the ports used to inject tracers when diffusivities at other ports are taken into account (r^2 = 0.99) and (b) median diffusivities for ports at the same depth that were not used to inject tracers (r^2 = 0.45).

It is usually more practical to use diffusivity models instead of in situ measurements, especially in projects that do not allow the use of convenient tracers. Modeling informed by in situ data is an optimal approach in this case. We calculated diffusivities using modeled soil air and moisture content to compare with results from diffusivity models. Models yielded poor fits (Fig. 7) and this failure is attributable to (i) the fact that moisture was not measured in the immediate vicinity of the ports, (ii) the natural variability of diffusivity due to soil macro features, and (iii) the poor ability of generic soil diffusivity models to predict diffusivity on a particular site without prior calibration.

Overall our results show that the single-port pulse injection method with SF_6 as an inert tracer provides a viable approach for obtaining reliable and quick estimates of gas diffusivity for a

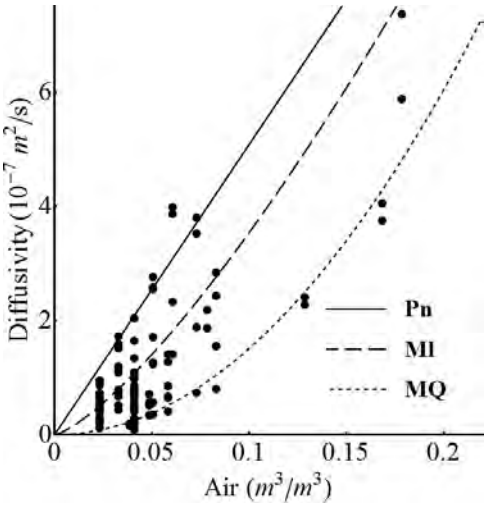

Fig. 7. Poor fit of common diffusivity models with measured sulfur hexafluoride diffusivities in this study. Lines are selected models of diffusivity: Penman 1940 (Pn), Millington 1959 (Ml), and Millington-Quirk 1961 (MQ).

particular site. Adjusting predictive diffusivity models with measurements for use at a specific site is simple and does not require a significant expenditure of resources. Using SF_6 as a tracer avoids complications related to the high solubility of N_2O and its production and perhaps consumption in a given soil.

Our method could be improved and better applied in other soils with more precise estimates of moisture and temperature, making them more informative to generic soil diffusivity models on the site of interest. With additional resources, the continuous-injection method is likely to provide more precise estimates of N_2O diffusivity for any given soil by achieving a stationary SF_6 concentration profile and simplifying analytical procedures. For general use, however, our method provides estimates that should be sufficient and an improvement over static models for parameterizing most quantitative biogeochemical models.

CONCLUSIONS

1. We found no evidence of N_2O consumption in our site either in summer or fall.

2. The point source single-port method with sparse measurements yielded reliable estimates of diffusivity; the inter-port method did not improve precision.

3. Diffusivity estimates were higher in rainfed than irrigated treatments during the summer measurements, likely due to lower soil moisture under rainfed conditions. Likewise, in the fall when there were no soil moisture differences between treatments at 36 and 60 cm, diffusivities were similar.

4. Measurements performed with SF_6 to estimate N_2O diffusivity were more appropriate than direct measurements with N_2O due to the incomplete equilibration of N_2O with soil water.

5. Our diffusivity estimates with modeled water content did not have strong agreement with published diffusivity models that are very sensitive to proper determination of the water content.

ACKNOWLEDGMENTS

We thank K. Kahmark and S. VanderWulp for help with sampling and laboratory analyses, and V. Shcherbak for help with figures. We also thank B. Basso, S.K. Hamilton, and A.N. Kravchenko for many helpful discussions and comments on earlier results.

REFERENCES

Allaire, S.A., and E. van Bochove. 2006. Collecting large soil monoliths. Can. J. Soil Sci. 86:885–896. doi:10.4141/S05-062

Allaire, S.E., J.A. Lafond, A.R. Cabral, and S.F. Lange. 2008. Measurement of gas diffusion through soils: Comparison of laboratory methods. J. Environ. Monit. 10:1326–1336. doi:10.1039/b809461f

Basso, B., J.T. Ritchie, P.R. Grace, and L. Sartori. 2006. Simulation of tillage systems impact on soil biophysical properties using the SALUS model. Italian J. Agron. 1:677–688.

Bruckler, L., B.C. Ball, and P. Renault. 1989. Laboratory estimation of gas-diffusion coefficient and effective porosity in soils. Soil Sci. 147:1–10. doi:10.1097/00010694-198901000-00001

Buckingham, E. 1904. Contributions to our knowledge of the aeration of soils. U.S. Dep. of Agriculture. Bureau of Soils, Washington, DC.

Cannavo, P., F. Lafolie, B. Nicolardot, and P. Renault. 2006. Modeling seasonal variations in carbon dioxide and nitrous oxide in the vadose zone. Vadose Zone J. 5:990–1004. doi:10.2136/vzj2005.0124

Clough, T.J., R.R. Sherlock, and D.E. Rolston. 2005. A review of the movement and fate of N_2O in the subsoil. Nutr. Cycling Agroecosyst. 72:3–11. doi:10.1007/s10705-004-7349-z

Crum, J.R., and H.P. Collins. 1995. KBS soils. W.K. Kellogg Biol. Sta. Long-Term Ecol. Res. Project, Michigan State Univ., Hickory Corners, MI. Available at http://lter.kbs.msu.edu/research/site-description-and-maps/soil-description/.

Del Grosso, S.J., W.J. Parton, A.R. Mosier, M.K. Walsh, D.S. Ojima, and P.E. Thornton. 2006. DAYCENT national-scale simulations of nitrous oxide emissions from cropped soils in the United States. J. Environ. Qual. 35:1451–1460. doi:10.2134/jeq2005.0160

Friedman, H.L. 1954. The solubilities of sulfur hexafluoride in water and of the rare gases, sulfur hexafluoride and osmium tetroxide in nitromethane. J. Am. Chem. Soc. 76:3294–3297. doi:10.1021/ja01641a065

Gevantman, L.H. 2010. Solubility of selected gases in water. In: D.R. Lide, editor, Handbook of chemistry and physics. 90th ed. CRC Press, Boca Raton, FL. p. 8–81.

Goldberg, S. D. and G. Gebauer. 2009. Drought turns a Central European Norway spruce forest soil from an N_2O source to a transient N_2O sink. Global Change Biol. 15:850-860.

Heincke, M., and M. Kaupenjohann. 1999. Effects of soil solution on the dynamics of N_2O emissions: A review. Nutr. Cycling Agroecosyst. 55:133–157. doi:10.1023/A:1009842011599

Jassal, R., A. Black, M. Novak, K. Morgenstern, Z. Nesic, and D. Gaumont-Guay. 2005. Relationship between soil CO_2 concentrations and forest-floor CO_2 effluxes. Agric. For. Meteorol. 130:176–192. doi:10.1016/j.agrformet.2005.03.005

Jin, Y., and W.A. Jury. 1996. Characterizing the dependence of gas diffusion coefficient on soil properties. Soil Sci. Soc. Am. J. 60:66–71. doi:10.2136/sssaj1996.03615995006000010012x

Kreamer, D.K., E.P. Weeks, and G.M. Thompson. 1988. A field technique to measure the tortuosity and sorption-affected porosity for gaseous-diffusion of materials in the unsaturated zone with experimental results from near Barnwell, South Carolina. Water Resour. Res. 24:331–341. doi:10.1029/WR024i003p00331

Lai, S.H., J.M. Tiedje, and A.E. Erickson. 1976. In-situ measurement of gas-diffusion coefficient in soils. Soil Sci. Soc. Am. J. 40:3–6. doi:10.2136/sssaj1976.03615995004000010006x

Lange, S.F., S.E. Allaire, and D.E. Rolston. 2009. Soil-gas diffusivity in large soil monoliths. Eur. J. Soil Sci. 60:1065–1077. doi:10.1111/j.1365-2389.2009.01172.x

Li, C.S., S. Frolking, and T.A. Frolking. 1992a. A model of nitrous-oxide evolution from soil driven by rainfall events.1. Model structure and sensitivity. J. Geophys. Res. Atmos. 97:9759–9776. doi:10.1029/92JD00509

Li, C.S., S. Frolking, and T.A. Frolking. 1992b. A model of nitrous-oxide evolution from soil driven by rainfall events. 2. Model applications. J. Geophys. Res. Atmos. 97:9777–9783. doi:10.1029/92JD00510

Lide, D.R. 2010. Definitions of scientific terms. In: D.R. Lide, editor, Handbook of chemistry and physics. 90th ed., CRC Press, Boca Raton, FL. p. 2–49.

Marshall, T.J. 1959. The diffusion of gases through porous media. J. Soil Sci. 10:79–82. doi:10.1111/j.1365-2389.1959.tb00667.x

Microsoft. 2012. Microsoft visual studio 2012. Microsoft, Redmond, WA.

Millington, R.J. 1959. Gas diffusion in porous media. Science 130:100–102. doi:10.1126/science.130.3367.100-a

Millington, R.J., and J.P. Quirk. 1960. Transport in porous media. Trans. 7th int. Congr. Soil Sci. 1:97–106.

Millington, R., and J.P. Quirk. 1961. Permeability of porous solids. Trans. Faraday Soc. 57:1200–1207. doi:10.1039/tf9615701200

Mokma, D.L., and J.A. Doolittle. 1993. Mapping some loamy Alfisols in southwestern Michigan using ground-penetrating radar. Soil Surv. Horiz. 34:71–77.

Moldrup, P., T. Olesen, P. Schjonning, T. Yamaguchi, and D.E. Rolston. 2000. Predicting the gas diffusion coefficient in undisturbed soil from soil water characteristics. Soil Sci. Soc. Am. J. 64:94–100. doi:10.2136/sssaj2000.64194x

Moldrup, P., T. Olesen, S. Yoshikawa, T. Komatsu, and D.E. Rolston. 2005. Predictive-descriptive models for gas and solute diffusion coefficients in variably saturated porous media coupled to pore-size distribution: I. Gas dlifusivity in repacked soil. Soil Sci. 170:843–853. doi:10.1097/01.ss.0000196769.51788.73

Nicot, J.P., and P.C. Bennett. 1998. Shallow subsurface characterization of gas transport in a playa wetland. J. Environ. Eng. 124:1038–1046. doi:10.1061/(ASCE)0733-9372(1998)124:11(1038)

Peaceman, D.W., and H.H. Rachford. 1955. The numerical solution of parabolic and elliptic differential equations. J. Soc. Ind. Appl. Math. 3:28–41. doi:10.1137/0103003

Penman, H.L. 1940. Gas and vapour movements in the soil I. The diffusion of vapours through porous solids. J. Agric. Sci. 30:437–462. doi:10.1017/S0021859600048164

Resurreccion, A.C., P. Moldrup, K. Kawamoto, S. Hamamoto, D.E. Rolston, and T. Komatsu. 2010. Hierarchical, bimodal model for gas diffusivity in aggregated, unsaturated soils. Soil Sci. Soc. Am. J. 74:481–491. doi:10.2136/sssaj2009.0055

Senthilkumar, S., B. Basso, A.N. Kravchenko, and G.P. Robertson. 2009. Contemporary evidence of soil carbon loss in the U.S. Corn Belt. Soil Sci. Soc. Am. J. 73:2078–2086. doi:10.2136/sssaj2009.0044

Syswerda, S.P., B. Basso, S.K. Hamilton, J.B. Tausig, and G.P. Robertson. 2012. Long-term nitrate loss along an agricultural intensity gradient in the Upper Midwest USA. Agric. Ecosyst. Environ. 149:10–19. doi:10.1016/j.agee.2011.12.007

Thomas, L.H. 1949. Elliptic problems in linear difference equations over a network. Watson Sci. Comput. Lab. Rep. Columbia University, New York.

van Bochove, E., N. Bertrand, and J. Caron. 1998. In situ estimation of the gaseous nitrous oxide diffusion coefficient in a sandy loam soil. Soil Sci. Soc. Am. J. 62:1178–1184. doi:10.2136/sssaj1998.03615995006200050004x

Weeks, E.P., D.E. Earp, and G.M. Thompson. 1982. Use of atmospheric fluorocarbons F-11 and F-12 to determine the diffusion parameters of the unsaturated zone in the southern high-plains of Texas. Water Resour. Res. 18:1365–1378. doi:10.1029/WR018i005p01365

Werner, D., P. Grathwohl, and P. Hohener. 2004. Review of field methods for the determination of the tortuosity and effective gas-phase diffusivity in the vadose zone. Vadose Zone J. 3:1240–1248.

Werner, D., and P. Hohener. 2003. In situ method to measure effective and sorption-affected gas-phase diffusion coefficients in soils. Environ. Sci. Technol. 37:2502–2510. doi:10.1021/es020101s

Wolfram Research. 2012. Wolfram Mathematica 9.0. Wolfram Research, Champaign, IL.